

# Thermal properties of plasma-sprayed tungsten deposits

Hyun-Ki Kang \*

Department of Materials Technology, Korea Institute of Machinery & Materials, 66 Sangnam-dong, Changwon, 641-010, South Korea

Received 24 March 2004; accepted 7 June 2004

## Abstract

Tungsten powder was plasma-sprayed onto a graphite substrate in order to examine the microstructures, porosities, and thermal conductivities of tungsten deposits. Tungsten was partially oxidized to tungsten oxide ( $\text{WO}_3$ ) after plasma spraying. Most pores were found in the vicinity of lamellar layers in association with oxidation. It was revealed that both tungsten oxide and the lamellar structure with pores have a significant influence on the electrical and thermal conductivity.

© 2004 Elsevier B.V. All rights reserved.

PACS: 65

## 1. Introduction

Tungsten has a body centered cubic structure (bcc), a high melting point (3420 °C), good erosion resistance to welding and spark, low vapor pressure ( $1.3 \times 10^{-7}$  Pa at  $T_{\text{melt}}$ ), high strength and dimensional stabilities at elevated temperatures, low thermal expansion coefficient ( $4.4 \times 10^{-6}/\text{K}$ ), and high thermal conductivity (180 W/mK). These prominent properties make tungsten a candidate for contact material and plasma facing components for the divertor region in International Thermonuclear Experimental Reactors (ITER). In addition, tungsten oxide ( $\text{WO}_3$ ) has been used in electronic devices, catalysts, and chemical sensors. According to Gillet et al. [1], the electrical conductivity of tungsten oxide can be changeable from the wide bandgap semiconductor state ( $\text{WO}_3$ ) to the conductor state ( $\text{WO}_2$ ). Smid et al. [2] reported comprehensive research into tungsten

armor and bonding to copper for plasma-interactive compounds. W-1% $\text{La}_2\text{O}_3$  exhibited a high recrystallization temperature, high thermal strength, and good machinability. However, shortcomings such as reduced thermal conductivities arise. Recently, Döring et al. [3] explored the processing of vacuum plasma-sprayed tungsten-copper composite coatings for high heat flux components. They solved the issue of reduced thermal conductivity by adopting a functionally gradient material that exhibits a smooth property transition (i.e. thermal expansion coefficient) from copper to tungsten. Moreau et al. [4] conducted an experiment on the thermal diffusivity of plasma-sprayed tungsten coatings. They concluded that the lower thermal diffusivity of plasma-sprayed tungsten coatings, compared to that of bulk tungsten, was attributed to the coating's lamellar structure. However, tungsten oxidation may have some influence on the thermal diffusivity ( $\alpha$ ), which determines the thermal conductivity ( $\kappa$ ) by the following equation:

$$\kappa = \rho_s C_p \alpha, \quad (1)$$

\* Tel.: +82 55 280 3308; fax: +82 55 280 3399.

E-mail address: [kanghyun6@yahoo.com](mailto:kanghyun6@yahoo.com)

where  $C_p$  is the specific heat and  $\rho_s$  is the sintered density.

Thus, it is useful to investigate the influences of both the coating's lamellar structure and tungsten oxidation on thermal diffusivity.

In the present study, plasma-sprayed tungsten deposition was carried out to explore the effects on thermal diffusivity and conductivity of the deposit. The microstructure and oxidation of the tungsten deposit were also discussed.

## 2. Experimental procedures

Tungsten feedstock powder (TaeguTec Ltd., Korea, 99.9%, <13.5  $\mu\text{m}$ ) was plasma-sprayed onto a graphite substrate ( $100 \times 120 \times 10 \text{ mm}^3$ ) in air using the Valu-Plaza™ thermal plasma spray system (40 kW), incorporating a 4 MP-Dual powder feed unit with an SG-100 gun (Praxair, USA) controlled by a computer program, which moved the gun in  $x$ - and  $y$ -directions at intervals of 3 mm. Table 1 shows the experimental parameters of the present thermal plasma spray. Argon gas was used as both the plasma and carrier gas. After plasma spraying, the deposits were detached from the substrates by the mechanism of thermal expansion mismatch at the interfaces between the deposits and substrates. Phase constituents of deposits was identified by a Rigaku X-ray diffractometer with Cu  $K\alpha$  radiation at 40 kV and 34 mA. A scanning electron microscope (JEOL 8600, Japan) with back-scattered electrons as well as a Nikon Epiphot 200 optical microscope, were utilized to examine the microstructure and porosity of the deposits after being polished with 1  $\mu\text{m}$  diamond paste. The thermal diffusivity and thermal conductivity were measured at an in-plane direction parallel to the deposit using a laser flash instrument (LFA-437, NETZSCH-Geraetebau GmbH, Korea Institute of Machinery and Materials) at room temperature. The electrical conductivity was measured at 10 sites on each specimen using the eddy current method. A Sigmascop SMP10 (Fischer Technology, Inc.) was used at a probe frequency of

Table 1  
Present plasma spraying parameters

Parameters/torch	SG-100
Input power (kW)	25, 27, 30
Input current (A)	500
Input voltage (V)	50, 54, 60
1st gas flow rate (Ar, l/min)	47.2
2nd gas flow rate (H <sub>2</sub> , l/min)	3.78, 7.08, 9.44
Carrier gas (Ar, l/min)	6.6
Powder feed rate (g/min)	25
Traverse rate (mm/s)	20
Spray distance (mm)	100

68 KHz after the sprayed deposits were ground to a thickness of 450  $\mu\text{m}$ .

## 3. Results and discussion

### 3.1. Microstructure observation

Fig. 1 shows the cross-section of a free-standing tungsten deposit plate. The thickness of the deposit plate was 0.8 mm. Generally, a dense deposit was observed. Several pores were found scattered in the vicinity of the coating's lamellar layers as shown in Fig. 2(a). It is seen that most of the sprayed tungsten particles were completely melted and deposited. As shown in Fig. 2(b), stacks of large lamellar layers with thicknesses of about 5  $\mu\text{m}$  are seen. Small intra-lamellar pores were observed, while large inter-lamellar pores were found. Dark areas at the inter-lamellar layer boundaries are attributed to tungsten oxide (WO<sub>3</sub>). This implies that most pores developed at the inter-lamellar layers in association with oxidation during plasma spraying.

### 3.2. Tungsten oxidation

Fig. 3 shows the phase constituents of the plasma-sprayed tungsten deposits. With an increase in input power, the level of the WO<sub>3</sub> peak increased. Hegetüs et al. [5] reported that WO<sub>2</sub> was observed after oxidizing alpha tungsten in moist hydrogen at about 740 °C. Their proposed reaction is expressed as follows:



Bigey et al. [6] identified various oxidation states of tungsten oxide using XPS technology. They concluded based on the observations (XPS, XRD) that the reduction took place as follows:

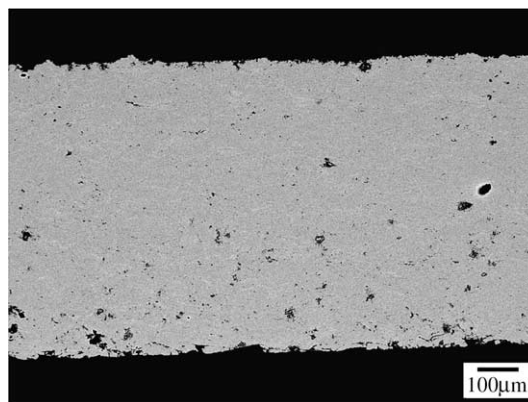


Fig. 1. SEM micrograph of cross-sectioned plasma-sprayed tungsten deposit.

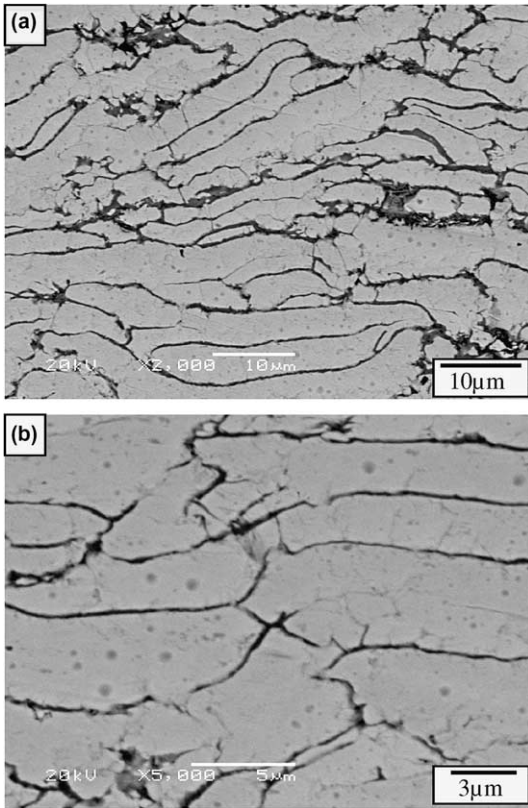


Fig. 2. SEM micrographs of plasma-sprayed tungsten deposit: (a)  $\times 2000$ ; (b)  $\times 5000$ .

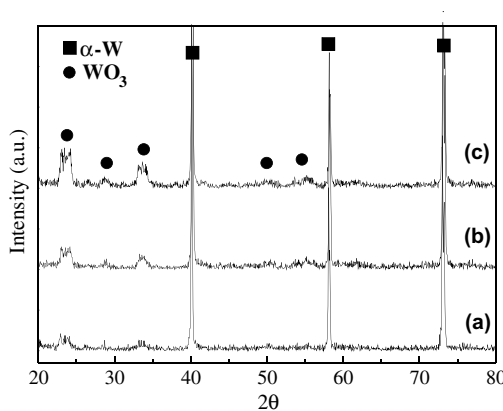
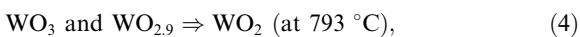
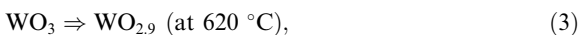


Fig. 3. XRD patterns of plasma-sprayed tungsten deposits along with different input powers: (a) 25; (b) 27; (c) 30 kW.



However, it is known that plasma spray uses high temperatures (5000–12000 °C) and high velocities (200–600 m/s) [7,8]. Thus, there is not enough resident time for the formation of such  $\text{WO}_x$ , due to the rapid solidification of liquid/semi-liquid droplets in the range of  $10^{5-7}$  K/s [9]. As a result, reactions (2)–(5) may not occur. When droplets impinge the substrate, the droplets’ temperatures rapidly decrease to near substrate temperatures due to the large temperature gradient between the plasma torch and the substrate, as reported by many researchers [7,10–12]. It seems that some small tungsten particles were oxidized to tungsten oxide vapor ( $\text{WO}_3$  (g)) in the high temperature plasma jet of approximately 3900 K and then became tungsten oxide ( $\text{WO}_3$ (g)) by rapid solidification [13].

### 3.3. Thermal and electrical properties

Fig. 4 shows the thermal diffusivity of plasma-sprayed tungsten deposits versus porosity. Although the level of the porosities gradually decreased, the thermal diffusivities did not increase correspondingly. At the input power of 30 kW, the value of the thermal diffusivity was dropped a little, comparing to that at 27 kW. According to Castro et al. [14], assuming no oxidation in the coatings, the thermal diffusivity increases with decreasing porosity. However, in the present case, the tungsten deposits were oxidized to  $\text{WO}_3$  as shown in Fig. 3. This indicates that oxidation has a significant influence on thermal diffusivity. The thermal diffusivity of bulk tungsten is about  $7 \times 10^{-5}$  m<sup>2</sup>/s. The measured values ( $\sim 3 \times 10^{-6}$  m<sup>2</sup>/s) were extremely lower than bulk tungsten’s value. This is attributed to the structural imperfections of the plasma-sprayed deposit, stacked individual lamellae with the presence of pores and oxides.

Fig. 5 shows the electrical and thermal conductivities versus porosities along with different input power levels. From the theoretical Eq. (1), it is noted that thermal conductivity increases with increasing material density.

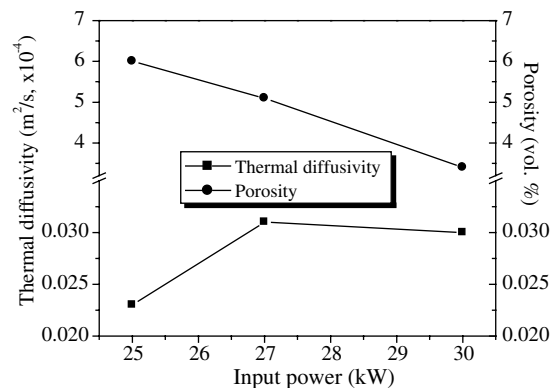


Fig. 4. Thermal diffusivity versus porosity.

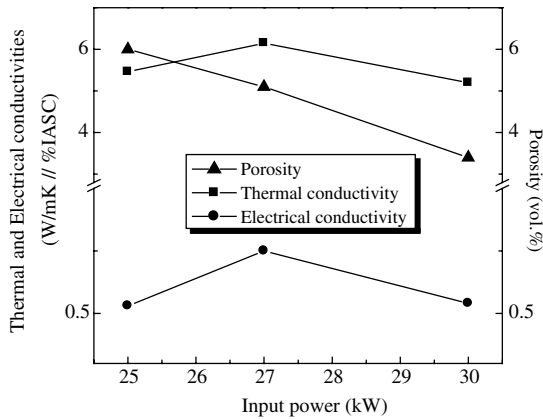


Fig. 5. Conductivity and porosity along with input power.

However, the present results show a different tendency, because pores and impurities (oxides) in the deposit limit inter-lamellar free electron movement. According to the Wiedemann–Franz law, the relationship between the electrical conductivity and thermal conductivity can be expressed as follows:

$$\sigma = \frac{N_f e^2 \tau}{m^*} = \frac{1}{\rho}, \quad (6)$$

$$\frac{\kappa}{\sigma T} = \frac{\pi^2 k_B^2}{3e^2}, \quad (7)$$

where  $\sigma$  is the electrical conductivity,  $\tau$  is the relaxation time,  $m^*$  is the effective mass,  $\rho$  is the electrical resistivity, and  $k_B$  is the Boltzmann constant. Thus, the electrical conductivity has the same tendency as the thermal conductivity.

#### 4. Conclusions

A free-standing plasma-sprayed tungsten plate was produced using an atmospheric plasma spray. Most of

the tungsten particles were melted and deposited on the graphite substrate. During plasma spraying, tungsten oxide ( $\text{WO}_3$ ) was formed by the rapid solidification of droplets. It was revealed that both tungsten oxide and the lamellar structure with pores have a significant influence on electrical and thermal conductivity. The tendency of the electrical conductivity was similar to that of the thermal conductivity. In order to protect against tungsten oxidation, it is suggested to plasma spray tungsten powder in vacuum or lower pressure chamber with inert gas.

#### References

- [1] M. Gillet, K. Mašek, C. Lemire, *Thin Solid Films* 444 (2003) 9.
- [2] I. Smid, M. Akiba, G. Vieider, L. Plöchl, *J. Nucl. Mater.* 263–285 (1998) 160.
- [3] J.-E. Döring, R. Vaßen, G. Pintsuk, D. Stöver, *Fusion Eng. Des.* 66–68 (2003) 259.
- [4] C. Moreau, P. Fargier-Richard, R.G. Saint-Jacques, P. Cielo, *Surf. Coat. Technol.* 61 (1993) 67.
- [5] É. Hegetüs, J. Neugebauer, M. Mészáros, *Int. J. Refract. Met. Hard Mater.* 16 (1998) 31.
- [6] C. Bigey, L. Hilaire, G. Maire, *J. Catalysis* 184 (1999) 406.
- [7] N. El-Kaddah, J. McKelliget, J. Szekeley, *Metall. Trans. B* 15 (1984) 59.
- [8] S. Paik, X. Chen, P. Kong, E. Pfender, *Plasma Chem. Plasma Process.* 11 (1991) 229.
- [9] R. Smith, R. Knight, *J. Met.* 47 (1995) 32.
- [10] E. Pfender, Y.C. Lee, *Plasma Chem. Plasma Process.* 5 (1985) 211.
- [11] P.C. Huang, J. Heberlein, E. Pfender, *Surf. Coat. Technol.* 73 (1995) 142.
- [12] E. Pfender, *Plasma Chem. Plasma Process.* 9 (1989) 167S.
- [13] H.-K. Kang, S.B. Kang, *Surf. Coat. Technol.* 182 (2004) 124.
- [14] R.G. Castro, A.H. Barlett, K.J. Hollis, R.D. Fields, *Fusion Eng. Des.* 37 (1997) 243.